Bradford, M. M. (1976) *Anal. Biochem. 72*, 248–254.
Brenner, D. G., & Knowles, J. R. (1981) *Biochemistry* (in press).
Brown, A. G., Butterworth, D., Cole, M., Hanscomb, G., Hood, J. D., & Reading, C. (1976) *J. Antibiot. 29*, 668–669.
Cartwright, S. J., & Coulson, A. F. W. (1979) *Nature (London) 278*, 360–361.
Charnas, R. L., Fisher, J., & Knowles, J. R. (1978) *Biochemistry 17*, 2185–2189.
Cohen, S. A., & Pratt, R. F. (1980) *Biochemistry 19*, 3996–4003.
Durkin, J. P., & Viswanatha, T. (1978) *J. Antibiot. 31*, 1162–1169.
Elson, S. W., & Oliver, R. S. (1978) *J. Antibiot. 31*, 586–592.
English, A. R., Retsema, J. A., Girard, A. E., Lynch, J. E., & Barth, W. E. (1978) *Antimicrob. Agents Chemother. 14*, 414–419.
Fisher, J., & Knowles, J. R. (1980) in *Enzyme Inhibitors as Drugs* (Sandler, M., Ed.) pp 209–218, Macmillan, London.
Fisher, J., Charnas, R. L., & Knowles, J. R. (1978) *Biochemistry 17*, 2180–2184.
Fisher, J., Belasco, J. G., Khosla, S., & Knowles, J. R. (1980) *Biochemistry 19*, 2895–2901.
Gordon, E. M., Chang, H. W., Cimarusti, C. M., Toeplitz, B., & Gougoutas, J. Z. (1980) *J. Am. Chem. Soc. 102*, 1690–1702.
Hammarström, S., & Strominger, J. L. (1975) *Proc. Natl. Acad. Sci. U.S.A. 72*, 3463–3467.
Howarth, T. T., Goodacre, J., & Ponsford, R. J. (1977) *Ger. Offen.* 2616088.
Kemal, C., & Knowles, J. R. (1981) *Biochemistry* (in press).
Knott-Hunziker, V., Orlek, B. S., Sammes, P. G., & Waley, S. G. (1979) *Biochem. J. 177*, 365–367.
Knott-Hunziker, V., Orlek, B. S., Sammes, P. G., & Waley, S. G. (1980) *Biochem. J. 187*, 797–802.
Labia, R., & Peduzzi, J. (1978) *Biochim. Biophys. Acta 526*, 572–579.
Marquet, A., Frère, J.-M., Ghuysen, J.-M., & Loffet, A. (1979) *Biochem. J. 177*, 909–916.
Matthew, M., & Hedges, R. W. (1976) *J. Bacteriol. 125*, 713–718.
Pratt, R. F., & Loosemore, M. J. (1978) *Proc. Natl. Acad. Sci. U.S.A. 75*, 4145–4149.
Reading, C., & Hepburn, P. (1979) *Biochem. J. 179*, 67–76.
Samuni, A. (1975) *Anal. Biochem. 13*, 17–26.
Stirling, I., & Elson, S. W. (1979) *J. Antibiot. 32*, 1125–1129.
Sykes, R. B., & Matthews, M. (1976) *J. Antimicrob. Chemother. 2*, 115–117.
Thomas, G. B. (1968) *Calculus and Analytical Geometry*, 4th ed., Addison-Wesley, Reading, MA.
Tomasz, A. (1979) *Annu. Rev. Microbiol. 33*, 113–137.
Wrigley, C. W. (1971) *Methods Enzymol. 22*, 559–560.

Methotrexate and Folate Binding to Dihydrofolate Reductase. Separate Characterization of the Pteridine and *p*-Aminobenzoyl Binding Sites by Resonance Raman Spectroscopy†

Y. Ozaki, R. W. King, and P. R. Carey*

ABSTRACT: By using 324- and 350.6-nm excitation, it is possible to obtain selectively the resonance Raman spectra of the *p*-aminobenzoyl and pteridine chromophores, respectively, within methotrexate (MTX) or folate. Thus, for a single ligand, by changing the wavelength for excitation, the geometric conformations of both chromophores can be monitored separately. Resonance Raman spectra are reported for MTX bound to dihydrofolate reductases from *Escherichia coli* and from *Lactobacillus casei*, in each case in the presence and absence of NADPH. Additionally, some data are presented for enzyme-bound folate. The resonance Raman data support the conclusions of other workers that MTX binds with its pteridine ring protonated while the pteridine ring within folate is bound as a neutral species. However, for MTX, marked differences exist between the electronic distribution in the protonated pteridine ring for the ligand free in solution and for the bound species. The rearrangement of the pteridine electrons over and above that accompanying protonation explains the absorption properties of bound MTX, and together with protonation may account in part for the high affinity of MTX for the enzyme. The resonance Raman spectra show that slight differences exist between the pteridine sites for MTX in the three dihydrofolate reductases studied while no differences could be detected among the *p*-aminobenzoyl sites. In each MTX–protein complex, however, there appears to be a marked change in the geometry of the amide group in the benzoyl linkage of MTX compared to the geometry found in the free ligand. The resonance Raman spectra of MTX bound to the enzymes were unchanged upon the addition of the cofactor NADPH, indicating that the cofactor does not bring about marked electron rearrangement in the bound ligands.

Dihydrofolate reductase (5,6,7,8-tetrahydrofolate: $NADP^+$ oxidoreductase, EC 1.5.1.3) catalyzes the NADPH-linked reduction of dihydrofolate to tetrahydrofolate. The inhibition of this enzyme by the drug methotrexate (MTX)[1] (Figure 1) is the source of methotrexate's therapeutic effectiveness in the treatment of childhood leukemia and of several other cancers. Although methotrexate bears an overall structural similarity to the substrates (Figure 1), the affinity of the inhibitor for

† From the Division of Biological Sciences, National Research Council of Canada, Ottawa, Canada K1A 0R6 (Y.O. and P.R.C.), and the National Institute for Medical Research, The Ridgeway, Mill Hill, London NW7 1AA, United Kingdom (R.W.K.). *Received October 27, 1980.* This is NRCC No. 19367.

[1] Abbreviations used: MTX, methotrexate; RR, resonance Raman; DHFR, dihydrofolate reductase; Bis-Tris, bis(2-hydroxyethyl)iminotris(hydroxymethyl)methane.

0006-2960/81/0420-3219$01.25/0

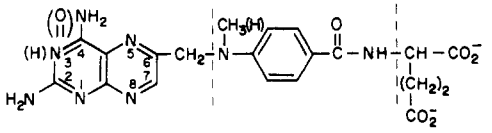

FIGURE 1: Structural formula for methotrexate (MTX). The formula for folate is obtained by substituting the atoms in parentheses. In MTX, the N(1) position has a pK of 5.7. In folate, the N(3) proton is removed at basic pH and has a pK of 8.1.

the enzyme is up to 10 000 times greater compared to that of the substrates. Several attempts have been made to understand this striking phenomenon at the molecular level. The substrates are 2-amino-4-oxopteridines whereas the most effective inhibitors, such as MTX, have 2,4-diamino substituents on a pteridine, pyrimidine, or related ring system (Baker, 1967; Blakeley, 1969; Roberts, 1978). Baker (1959, 1967) and Pullman and co-workers (Collin & Pullman, 1964) drew attention to the increased basicity of N(1) and of the 2-NH_2 group in 2,4-diaminopteridines compared to 2-amino-4-oxopteridines, and Baker (1959, 1967) suggested that the 2,4-diamino compounds bind to the active site in the protonated form. This additional coulombic energy was proposed as the source of the greater affinity of the inhibitors for the enzyme. Support for this concept came from absorbance difference spectra of MTX bound to dihydrofolate reductase from various sources (Erickson & Matthews, 1972; Poe et al., 1974, 1975; Hood & Roberts, 1978), from resonance Raman (Saperstein et al., 1978) and Raman (Durig et al., 1980) spectroscopic studies, and from X-ray crystallographic studies which show that the carboxylate group of Asp-27 is in close proximity to N(1) of MTX in the complex between MTX and dihydrofolate reductase from *Escherichia coli* (Matthews et al., 1977, 1978). In a recent absorption spectroscopy study, however, Hood & Roberts (1978) compare the binding of MTX and folate to the enzyme from *Lactobacillus casei* and conclude that although the pteridines of MTX and folate are protonated and neutral, respectively, upon binding only one-third of the additional binding energy of the MTX can be ascribed to the differences in charge state. One of the objectives of the present study was to investigate further at the molecular level the reasons for these differences in ligand–enzyme affinity.

In the present work, the binding of MTX and folate to dihydrofolate reductase from two sources is studied by resonance Raman spectroscopy. This technique provides vibrational spectra of chromophores at concentrations in the range of 10^{-4}–10^{-6} M in biological sites (Carey, 1978). Since vibrational spectra are sensitive to the disposition of electrons within chemical bonds, the resonance Raman spectra provide detailed information on the chemistry within and the environment surrounding the chromophore. The sources of the enzyme used in this study are *L. casei* and *E. coli*. *L. casei* dihydrofolate reductase is a single protein (Dann et al., 1976), while the enzyme purified from *E. coli* B RT500 is a mixture of two isoenzymes (Baccanari et al., 1977). These isoenzymes, designated form I and form II, differ only by replacement of a leucine in form I by an arginine in form II (D. Stone, unpublished experiments). This single amino acid change causes major differences in the affinity constant for inhibitors (with changes of up to a factor of 100 in K_a values), but not for coenzyme or substrates (Cayley et al., 1980). Folate binds weakly to form a 1:1 binary complex with *L. casei* dihydrofolate reductase ($K_a = 10^5$ M^{-1}; Hood & Roberts, 1978) while the *E. coli* isoenzymes form rather tighter complexes (form I, $K_a = 6 \times 10^5$ M^{-1}; form II, $K_a = 3 \times 10^6$ M^{-1}; Cayley et al., 1980). However, MTX binds very tightly in both the binary and ternary complexes, with $K_a > 10^8$ M^{-1} in each case (Hood & Roberts, 1978; Cayley et al., 1980; Dunn & King, 1980).

Experimental Procedures

The preparation, purification, and isolation of the two isoenzymatic forms of dihydrofolate reductase from *E. coli* B RT500 (the organism was a generous gift from Dr. J. J. Burchall, Burroughs-Wellcome) were carried out as described in Cayley et al. (1980). The isoenzymes are referred to as form I and form II, and these are the same isoenzymatic names as are used by Cayley et al. The preparation and purification of dihydrofolate reductase from *L. casei* MTX/R were carried out following the procedures described in Dann et al. (1976).

The purified enzymes were stored at −15 °C as ca. 1.0-mg lyophilized aliquots in sealed ampules under nitrogen. Before use, the ampules were opened, and buffer solution was added to give the required enzyme concentration, pH, and KCl concentration. In addition, 1.0 mM dithiothreitol was added to solutions of the *E. coli* isoenzymes to prevent polymerization (Baccanari et al., 1977). The enzyme samples were then allowed to stand at 4 °C for 16 h before use, since the catalytic and binding properties of the reconstituted enzymes are not fully developed until this time has elapsed (R. W. King, unpublished experiments). Enzyme concentration was determined by MTX titration of enzyme fluorescence and MTX titration of enzymatic activity.

Buffer solutions used were as follows: pH 5.0, 15 mM acetate and 500 mM KCl; pH 7.0, 15 mM Bis-Tris-HCl and 500 mM KCl; pH 7.5, 15 mM Tris-HCl and 500 mM KCl; pH 13.0, 0.1 N NaOH. NADPH and folic acid were obtained from Sigma Chemical Co. Methotrexate was obtained from Nutritional Biochemical Corp.; *p*-(dimethylamino)benzoylglutamate was a gift from Dr. B. Birdsall, National Institute for Medical Research, Mill Hill, U.K.

All experiments involving enzyme were carried out by using 1 mol of ligand/mol of enzyme, and the enzyme concentration was approximately 55 μM. At these concentrations, at pH 7.0, even the weakly binding folate saturates 70% of the enzyme in the binary complex with the *L. casei* enzyme.

Absorption spectra were measured by using a Cary 118 spectrophotometer. The 324- and 350.6-nm laser lines used for Raman excitation were from a Coherent Radiation 3000K laser, and the UV laser lines were dispersed by two Pellin Broca prisms. Typically, 40–70 mW of laser power was used. The Raman spectrum was analyzed by a Spex 0.5-m double monochromator equipped with direct current detection. A spectral slit of ~ 10 cm^{-1} was used to record each spectrum. The RR spectra shown are taken directly from a strip chart recorder; no data manipulation, such as signal averaging or subtraction of spectra, was carried out. For the obviation of problems due to photodegradation, the RR spectra were obtained by using a flow system for measurements not involving enzyme (B. A. E. MacClement, R. G. Carriere, D. J. Phelps, and P. R. Carey, unpublished experiments) and a rotating Raman cell for enzyme–ligand solutions. The absorption spectra before and after recording the Raman spectrum were identical.

Results and Discussion

Separate Probing of the Pteridine and Aminobenzoyl Binding Sites. (*i*) *Aminobenzoyl Group.* For both MTX and folate, the resonance Raman spectra obtained by using 324- and 350.6-nm excitation are essentially due to the aminobenzoyl chromophore alone or the pteridine chromophore alone, respectively. Thus, by changing the excitation wavelength, it is possible to probe selectively the pteridine or am-

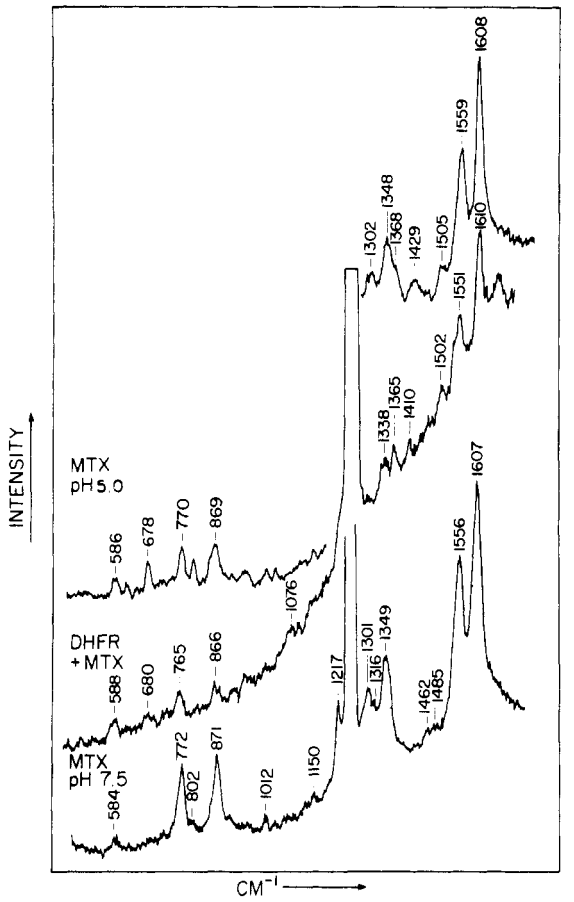

FIGURE 2: Resonance Raman spectra (324-nm excitation) of MTX: (top) 5.5×10^{-5} M in aqueous solution, pH 5.0 [pteridine N(1) protonated]; (center) bound to dihydrofolate reductase from *E. coli* I, 5.5×10^{-5} M in enzyme and ligand, pH 7.0; (bottom) 5.5×10^{-5} M in aqueous solution, pH 7.5, (pteridine neutral). For spectral conditions, see Experimental Procedures. The intense line at 1239 cm^{-1} and the line at 802 cm^{-1} are laser plasma lines.

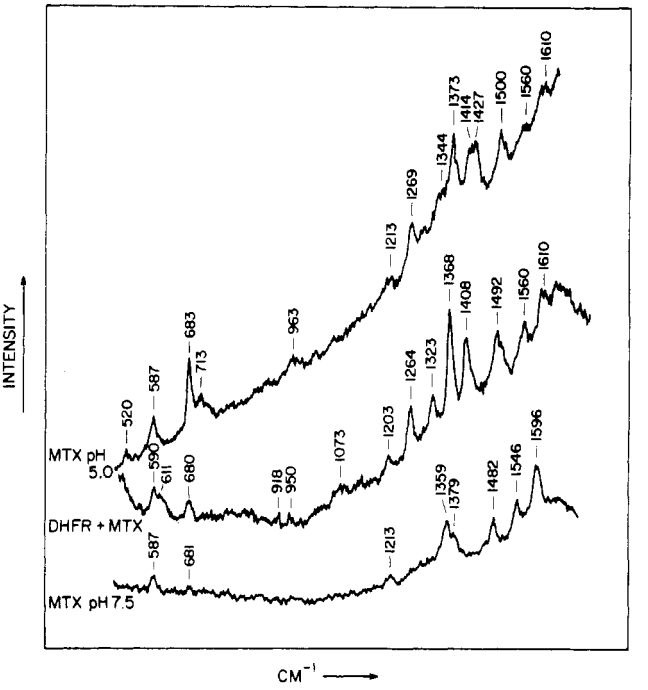

FIGURE 3: Resonance Raman spectra (350.6-nm excitation) of MTX: (top) 5.5×10^{-5} M in aqueous solution, pH 5.0 [pteridine N(1) protonated]; (center) bound to dihydrofolate reductase from *L. casei*, 5.5×10^{-5} M in enzyme and ligand, pH 7.0; (bottom) 5.5×10^{-5} M in aqueous solution, pH 7.5 (pteridine neutral). For spectral conditions, seen Experimental Procedures.

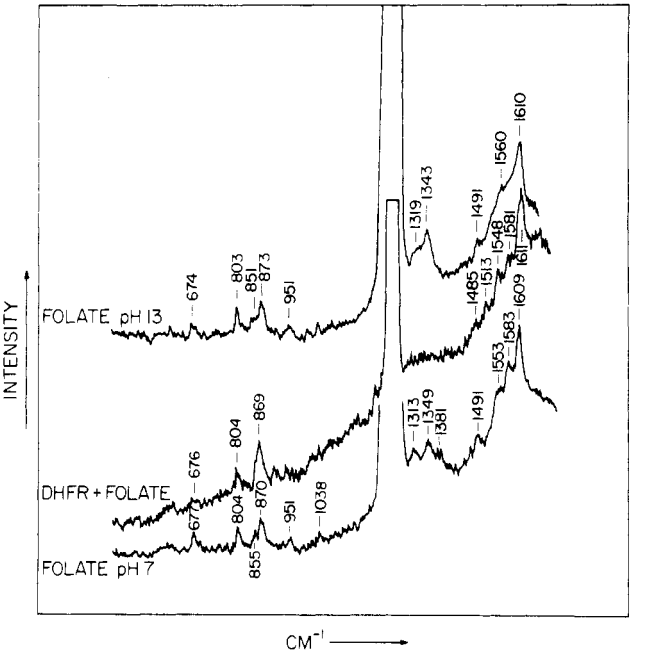

FIGURE 4: Resonance Raman spectra (324-nm excitation) of folate: (top) 4.4×10^{-5} M in aqueous solution, pH 13.0 (pteridine ionized); (center) bound to dihydrofolate reductase from *E. coli* II, 5.5×10^{-5} M in enzyme and ligand, pH 7.0; (bottom) 4.4×10^{-5} M in aqueous solution, pH 7.0 (pteridine neutral). For spectral conditions, see Experimental Procedures. The intense line at 1239 cm^{-1} is a laser plasma line.

inobenzoyl binding sites within the enzyme–ligand complexes. The "switching" of the RR spectra can be seen by comparing the RR spectra of MTX recorded by using 324-nm excitation (Figure 2) with the spectra of the same species recorded with 350.6-nm excitation (Figure 3). The main features in the 324-nm excited RR spectrum of MTX are unchanged by the protonation of the pteridine ring upon going from pH 7.5 to 5.0. Thus, there are no apparent changes in the positions of the bands at 1608, 1559, 1348, 1302, 869, and 770 cm^{-1}. These bands are missing or at best very weak in the corresponding 350.6-nm spectra. Peaks appear in similar positions in the 324-nm excited RR spectra of folate (see especially Figure 4, top) with the exception that the 770-cm^{-1} feature appears to have shifted to 803 cm^{-1}. Moreover, peaks at 1614, 1562, 1358, 1304, 872, and 758 cm^{-1} were observed in the 324-nm excited RR spectrum of the model compound *N*-[*p*-(dimethylamino)benzoyl]-*N*-methylglutamate (data not shown). The data taken together associate the bands at 1608, 1559, 1348, 1302, 869, and 770 cm^{-1} with vibrations involving the aminobenzoyl moiety in MTX, with the same conclusion holding for folate upon replacing the 770-cm^{-1} band by the folate feature at 804 cm^{-1}. (The feature seen near 800 cm^{-1} in the spectra in Figure 2 is probably due to a laser plasma line whereas the 804-cm^{-1} feature in Figure 4 contains a major contribution from a folate Raman band). Assignments of these peaks to well-defined group frequencies is not trivial and would require an independent spectroscopic study involving model compounds and their isotopically substituted analogues. However, the following comments can be made. The 1608-cm^{-1} band can almost certainly be assigned to a ring mode of a 1,4-disubstituted benzene, in agreement with an earlier assignment (Saperstein et al., 1978). The shift of the 770-cm^{-1} band in MTX to 804 cm^{-1} in folate indicates that these features are due to a vibrational mode which involves displacement of atoms in the amino function. In a further attempt to obtain a qualitative understanding of assignments, the spectra of MTX and folate were obtained in D_2O by using 324-nm ex-

citation. In D_2O, the amide NH within the benzamide moiety becomes ND in both ligands, and the amino NH of folate becomes ND. For both ligands, the bands at 1608, 869, 770 (MTX), and 804 cm^{-1} (folate) are unchanged by these isotopic substitutions (data not shown). Moreover, the band near 1560 cm^{-1} appears to be unaffected, although this conclusion is less definitive due to the broad nature of the peak for folate and an overlapping feature in the spectrum of MTX in D_2O (not shown). It is thus unlikely that the 1560-cm^{-1} band contains a major contribution from an amide II mode, and this conclusion receives some support from considering the 324-nm excited Raman spectra of the model compound *N*-methylbenzamide (data not shown). Importantly, in D_2O solution, there are large shifts in the 1348- and 1302-cm^{-1} peaks in the case of both ligands, and the 1220–1380-cm^{-1} region has no peaks in the RR spectra recorded in D_2O solution. Thus, the bands at 1348 and 1302 cm^{-1} involve motions of the amide hydrogen atom and can be used to probe interactions about the amide moiety.

It is apparent, then, that modes due to ring vibrations, and connected with amide and possibly amino vibrations of the *p*-aminobenzoyl group, appear in the 324-nm excited RR spectra. In other words, the chromophore, for the purposes of RR enhancement with 324-nm excitation, extends between the dashed lines shown in Figure 1. The weak band near 678 cm^{-1} appearing in the 324-nm excited RR spectra of MTX probably originates from the pteridine chromophore.

(ii) Pteridine Group. With 350.6-nm excitation, the features in the RR spectra of MTX and folate are almost exclusively from the pteridine chromophore. The intense bands in the spectrum of MTX at pH 5.0 obtained by using 350.6-nm excitation (Figure 3, top) are weak or missing in the 324-nm excited spectrum (Figure 2, top). Moreover, the same intense bands undergo large shifts when the pH is changed to 7.5, where the pteridine ring becomes electrically neutral (N-1 has a p*K* of 5.7 (Poe, 1973)], and also upon dissolving in D_2O at pH (measured) 5.0 (data not shown), where the amino group protons and the $-N(1)H^+$ proton will be exchanged. By consideration of these data, the bands in Figure 3 (top) at 683, 1269, 1373, 1414, 1427, and 1500 cm^{-1} are assigned to pteridine ring modes, some of which contain contributions from vibrations of the peripheral ring substituents. The mode near 585 cm^{-1} appears in all the spectra in Figures 2 and 3 and may be due to either the pteridine or the aminobenzoyl chromophore. The normal modes of the pteridine ring giving rise to the features seen, for example, in Figure 3 (top) contain, in all likelihood, contributions from many atomic vibrations. For this reason, we cannot assign the RR features to group frequencies. By comparing the spectra of MTX in H_2O and D_2O, we can, however, identify features that are specially sensitive to changes in motion, and therefore the environment surrounding the –NH protons. The region between 550 and 750 cm^{-1} is markedly changed upon going to D_2O; the features seen in Figure 3 (top) at 587, 683, and 713 cm^{-1} are replaced in D_2O by a band of medium intensity at 738 cm^{-1}, an intense band at 668 cm^{-1}, and a weak band at 574 cm^{-1}. However, the greatest spectral change is seen in the 1340–1450-cm^{-1} region. In D_2O, this spectral region becomes very similar to that shown in Figure 3 (center) for the bound MTX; namely, there are two intense modes which appear for free MTX in D_2O at 1377 and 1414 cm^{-1}, and there is no evidence for the features appearing at 1344 and 1427 cm^{-1} in Figure 3 (top). The conclusions concerning the origin of the bands in the 324- and 350.6-nm excited RR spectra are summarized in Table I.

Table I: Comments on the Features Appearing in the 324- and 350.6-nm Excited RR Spectra of MTX

324 nm		350.6 nm	
pH 5.0	pH 7.5	pH 5.0	pH 7.5
586[a]	584, PAB[b] or PT	587, PAB or PT	587, PAB or PT
678	PT	683, PT	
770	772, PAB	713, PT	
869	871, PAB		
1302	1301, PAB amide	1269, PT	1359, PT
1348	1349, PAB amide	1373, PT	1379, PT
1368		1414, PT	
1429	PT?	1427, PT	
1505	PT?	1500, PT	1482, PT
1559	1556, PAB	1560, PAB	1546, PT
1608	1607, PAB	1610, PAB	1596, PT

[a] All values in cm^{-1}. [b] PAB and PT represent the features associated with *p*-aminobenzoyl and pteridine chromophores, respectively.

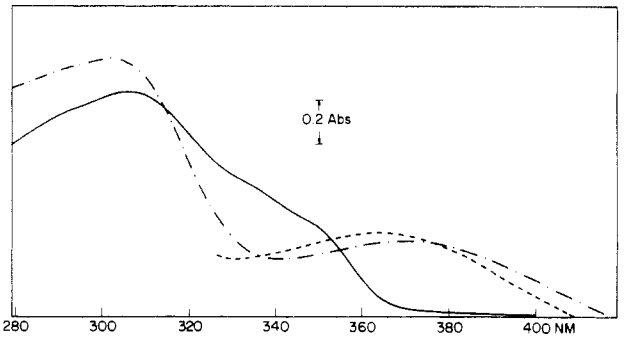

FIGURE 5: Absorption spectra of 5.3×10^{-5} M methotrexate, pH 1.0 (—) and pH 7.0 (–·–), and 4.4×10^{-5} M folate, pH 13.0 (- - -).

Relation of the RR Spectra to the Absorption Spectra. An intensity-enhanced (i.e., resonance) Raman spectrum is obtained when the wavelength of the laser light used to excite the spectrum lies within an absorption band of a chromophore. If the absorption band is due to a favorable $\pi \rightarrow \pi^*$ transition, the Raman intensity due to certain vibrational modes within the chromophore may be increased by a factor of 10^4–10^5. The absorption spectra of MTX at pH 1.0 and 7.0 are shown in Figure 5, and it is apparent from the preceding RR results and by considering the absorption spectra of model compounds that in the neutral species the pteridine chromophore makes the major contribution to the absorption band with λ_{max} near 370 nm (Figure 5) while the *p*-aminobenzoyl moiety makes the major contribution to the feature with λ_{max} near 306 nm. Upon protonation, the 370-nm pteridine band blue shifts to the 340-nm region. The wavelengths used to excite the RR spectra, 324 and 350.6 nm, are thus favorably disposed to selectively enhance the RR spectra of the aminobenzoyl and pteridine chromophores, respectively, for both the protonated and neutral species of the pteridine within MTX.

The insight that the combined RR and absorption data can provide into the electron distribution in a chromophore is further illustrated by a comparison of the spectra of pteridine within neutral MTX and within ionized folate. The absorption spectra of the pteridine moieties in these compounds are similar, with λ_{max} at 371 and 365 nm for MTX at pH 7 and for folate at pH 13, respectively (Figure 5). This resemblance is strongly reinforced by the RR data. The 350.6-nm excited RR spectrum of MTX at neutral pH (Figure 3, bottom) bears a close overall correspondence to that of folate at pH 13 (Figure 6, top). The spectral similarities reflect the similar electron distributions within the two pteridine analogues, I and

II. Thus, in MTX, I resembles the predominant canonical

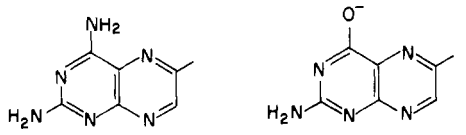

I II

form in ionized folate, namely, II. This, in turn, is because the $-NH_2$ and $-O^-$ groups have similar electrical properties, as is reflected by their Hammett parameters, for example. The close similarities of the RR spectra of chromophores containing either the $-NH_2$ or the $-O^-$ group have been noted before in the case of certain azobenzenes (Kumar et al., 1976; Kumar & Carey, 1977).

Ionization States and Interaction of Bound MTX and Folate. (*i*) *MTX.* Since the 350.6-nm excited RR spectrum of MTX yields data exclusively on the pteridine ring, we can focus attention on the latter moiety by comparing in Figure 3 the 350.6-nm excited spectrum of bound MTX with those of unbound MTX wherein the majority of the pteridines are protonated (pH 5) or unprotonated (pH 7.5). For the free molecule, gross changes occur in the RR spectrum upon protonation of the pteridine, indicating that substantial electron reorganization occurs in the ring. There is a general similarity between the spectrum of bound MTX (Figure 3, center) and that of the protonated species (Figure 3, top), supporting the conclusion arrived at by earlier workers by using absorption [Hood & Roberts (1978) and references cited therein] and RR spectroscopy (Saperstein et al., 1978) that the pteridine ring is protonated upon binding. The spectra in Figure 3 should agree closely with the RR data of Saperstein et al. (1978), who used 363.8-nm excitation, but unlike these authors we did not observe a band at 659 cm^{-1} unique to the MTX–enzyme complex. A major difference in conditions between the two sets of experiments is that Saperstein et al. (1978) employed concentrations of 5×10^{-3} M in the complex whereas our data are for concentrations of 5.5×10^{-5} M. Furthermore, the spectra shown in the present work are taken directly from a strip chart recorder connected to the direct current detection system whereas the data of Saperstein et al. were subject to data manipulation. The correspondence in Figure 3 between bound MTX and the free species at pH 5 is not exact, indicating that the enzyme–MTX interactions perturb the distribution of electrons in the bound pteridine chromophore over and above that due to protonation, and this topic is taken up in the following section. Particularly striking is the appearance of the 1323-cm^{-1} feature and the lack of the 1427-cm^{-1} band in the spectrum of the bound MTX and the difference in intensity of the 680-cm^{-1} feature (Figure 3, center). Since similar changes are seen when MTX is dissolved in D_2O (above), these differences between the spectra in the top and center of Figure 3 are taken to indicate that strong interactions occur between the protein and one or more of the pteridine $-NH_2$ or NH^+ groups. Good candidates are the hydrogen bonds, between the 2- and 4-amino groups with O_γ of Thr-116 and the backbone carbonyl of Leu-4, respectively, which have been characterized in an X-ray crystallographic study (Matthews et al., 1978). Additionally, the same study identified the close proximity of the side-chain carboxyl of Asp-26 to N(1) of bound methotrexate. Such interactions could change the vibrational coupling between ring and –NH modes in an analogous manner to the changes experienced upon deuteration.

Protein–ligand interactions about the *p*-aminobenzoyl group can be monitored by using 324-nm excitation for Raman

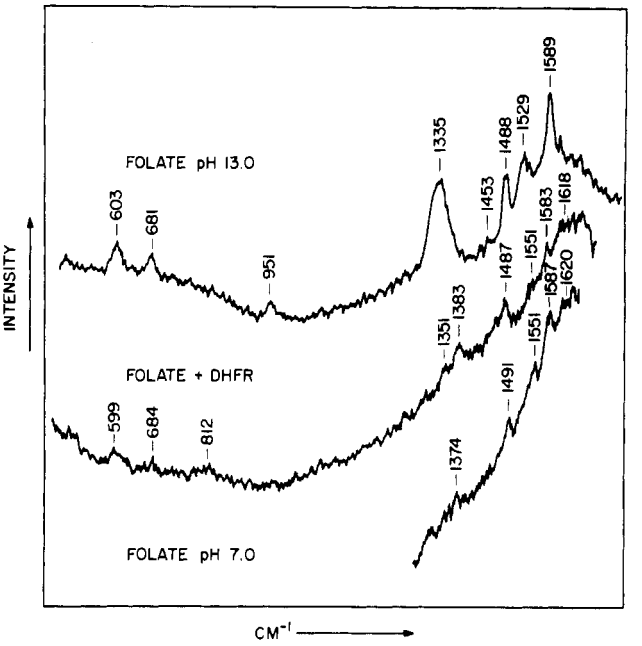

FIGURE 6: Resonance Raman spectra (350.6-nm excitation) of folate: (top) 4.4×10^{-5} M in aqueous solution, pH 13.0 (pteridine ionized); (center) bound to dihydrofolate reductase from *E. coli* II, 5.5×10^{-5} M in enzyme and ligand, pH 7.0; (bottom) 4.4×10^{-5} M in aqueous solution, pH 7.0 (pteridine neutral). For spectral conditions, see Experimental Procedures.

scattering. The majority of the intense features in Figure 2 are unchanged by going from pH 5.0 to pH 7.5 or by binding to the enzyme. However, the 1559-cm^{-1} feature of free MTX at pH 5.0 does shift to 1551 cm^{-1} upon binding to DHFR. The features at 1302 and 1348 cm^{-1} (Figure 2, top) are also unaffected by the change in pH, but they shift markedly in the spectrum of bound MTX. These bands were assigned above, by comparing RR spectra taken in H_2O and D_2O, to modes involving the amide group. The spectral differences between free MTX and the bound ligand in the 1300–1350-cm^{-1} region (Figure 2, top, bottom, and center) are therefore taken as evidence of a marked change in the chemical nature of the amide linkage in the enzyme-bound form of MTX. The change in the amide bonds could result either from strong protein–ligand interactions or from the removal of amide–solvent interactions. There is, at present, no X-ray crystallographic evidence for strong, directional protein–ligand forces, from, e.g., hydrogen bonding or charged amino acid side chains, about MTX's amide function. Hence, the preferred interpretation is that the spectral changes are brought about by the removal, upon binding, of the solvent shell around the amide group. Quantum mechanical calculations (Scheiner & Kern, 1977) provide support for this interpretation since they show that desolvation of the amide does result in considerable electron redistribution. Overall, this finding indicates that marked changes in the electron distribution in ligand groups can be caused by the exclusion of H_2O molecules in a hydrophobic pocket and that specific protein–ligand interactions are not an essential requirement to bring about changes in ligand properties.

(*ii*) *Folate.* The p*K* of the proton on the N(3) ring position of folate (Figure 1) is 8.38 (Poe, 1973), with the ring assuming a negative charge at higher pH. For the chromophoric part of the molecule, this is the only p*K* near physiological pH [e.g., the N(1) position of the pteridine has a p*K* near 2.0]. The RR data for folate are not as good in quality as those for MTX. However, the following points may be noted: in the 324-cm excited RR spectra of folate (Figure 4), the features

near 804, 872, 1315, 1345, 1560, and 1610 cm^{-1} are prominent and are essentially unaffected by the ionization of the N(3) proton in the pteridine ring [compare Figure 4, top, with Figure 4, bottom). In keeping with the assignments made for MTX, each of these bands is associated with the *p*-aminobenzoyl chromophore, with the 1315- and 1345-cm^{-1} peaks being assigned to modes involving the amide function. As in the case of MTX, most of the aminobenzoyl modes are unchanged by binding to DHFR (Figure 4, center). However, there does appear to be a change in the band profile in the 1350-cm^{-1} region, and again, as in the case of MTX, this is taken as evidence of perturbation to the structure of the folate amide group. The shoulder near 1580 cm^{-1} and the peak near 680 cm^{-1} in the spectra in Figure 4 are probably due to pteridine modes.

The 350.6-nm excited RR spectra of folate are of poor quality (Figure 6), but it is apparent that in the disposition of the pteridine features near 1375, 1490, and 1585 cm^{-1} the spectrum of bound folate most closely resembles that of the free species with the pteridine ring neutral. Therefore, in agreement with the conclusions reached by other methods (Baker, 1959, 1967; Hood & Roberts, 1978), the RR data indicate that no change occurs in the state of ionization of the pteridine group of folate on binding to DHFR.

Comparison of MTX and Folate Binding. The RR data offer some clues as to why MTX has a greater affinity than folate for DHFR. Hood & Roberts (1978), on the basis of absorption spectral studies, concluded that only one-third of the differences in binding energies of these two ligands could be accounted for by the fact that the pteridine moiety binds in the protonated form in MTX but in the neutral form in folate. By use of 324-nm excitation for the RR spectra to focus on the aminobenzoyl binding site, no discernable differences could be detected between the mode of binding of the aminobenzoyl in MTX or folate. There are, however, striking differences in the way in which the electrons in the pteridine chromophore rearrange when either MTX or folate binds to the enzymes. This is evident by comparing the RR spectra in Figures 3 and 6 obtained by using 350.6-nm excitation. These spectra show that little electron rearrangement occurs in the folate pteridine group upon binding at neutral pH since the spectra of the bound and unbound species at pH 7.0 are quite similar. However, for MTX, the pteridine moiety undergoes substantial electron rearrangement in the binding site since there are major differences in the spectra of the bound and unbound species near neutral pH (Figure 3). Importantly, there is evidence for a change in the spectrum of the bound moiety over and above that due to protonation. Therefore, the electron distribution in the protonated pteridine of enzyme-bound MTX only resembles that of the protonated free species to a degree. Binding site–pteridine interactions for MTX bring about a redistribution of electron density beyond that caused simply by protonation.

Charlton et al. (1979) have shown that the orientation of the pteridine ring of folate in the ternary complex is substantially different from the orientation of the pteridine ring of MTX. It is likely that the ring is rotated through 180° about its long axis as first suggested for dihydrofolate by Matthews et al. (1978). This differential effect of binding on the electron-density distribution in the pteridine ring of folate and MTX may well be a further manifestation of this orientation difference.

In summary, there appears to be little change in the electronic structure of the folate pteridine group upon binding whereas the pteridine group of MTX becomes protonated and

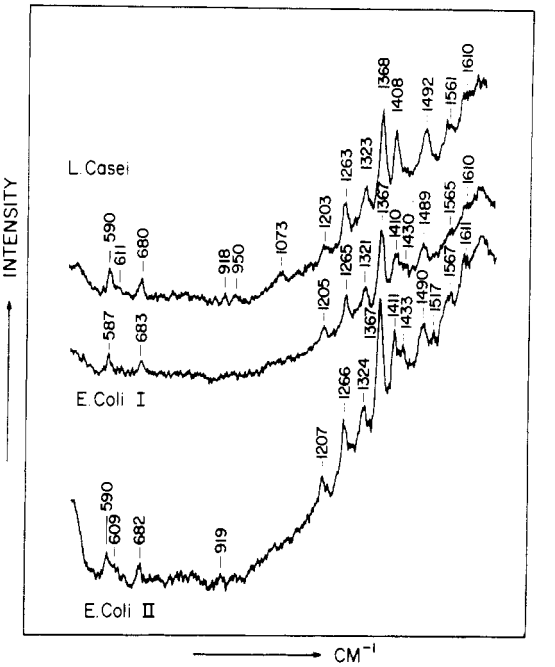

FIGURE 7: Comparison of the 350.6-nm excited resonance Raman spectra of methotrexate bound to dihydrofolate reductase from three sources, 5.5×10^{-5} M in enzyme and ligand, pH 7.0. For spectral conditions, see Experimental Procedures.

in addition undergoes a further electron rearrangement. Since the latter rearrangement must reflect forces between the ligand and the active site, we suggest that it increases the favorable binding energy and accounts, at least in part, for the additional portion of binding energy [i.e., unaccounted for by MTX pteridine protonation (Hood & Roberts, 1978)] for MTX binding to enzyme compared to folate binding to enzyme. It is the overall electronic complementarity of the pteridine moiety in MTX to the enzyme's active site, of which protonation is but a part, that is therefore proposed to account for the observed differences in MTX and folate binding constants. Finally, given the differences between the RR spectra of free protonated MTX (Figure 3, top) and the enzyme-bound species (Figure 3, center), we would not expect the absorption spectra of the pteridine group to be identical in the two cases, and such a disparity has been reported by other workers (Hood & Roberts, 1978).

Comparison of the MTX Binding Sites in DHFR from E. coli and L. casei. Figure 7 compares the 350.6-nm excited RR spectra of MTX bound to *E. coli* form I, *E. coli* form II, and *L. casei*, and therefore probes the pteridine binding sites in these enzymes. The spectra in Figure 7 are generally alike, but reproducible differences occur near 1430, 1517, and 1565 cm^{-1}. The isoenzymes from *E. coli* show a feature near 1430 cm^{-1} in the RR spectrum of the MTX–enzyme complex, but this is either weak or absent in the corresponding spectrum from the *L. casei* complex. On the basis of the sensitivity of the 1430-cm^{-1} feature to deuterium substitution (above), the differences in this feature among the three enzyme–MTX complexes are taken to indicate that differences in active site–pteridine interactions occur for one of the $-NH_2$ groups or the $-NH^+$ group. Additional differences among the three spectra in Figure 7 are the appearance of a weak extra band at 1517 cm^{-1} and small shifts in peak positions, most notably in the feature at 1567 cm^{-1} (Figure 7 and in the complex with NADPH, Figure 8), most clearly seen in the complex involving *E. coli* form II. The origin of these bands is unclear, but it is likely that the 1430- and 1517-cm^{-1} features are associated with the pteridine nucleus.

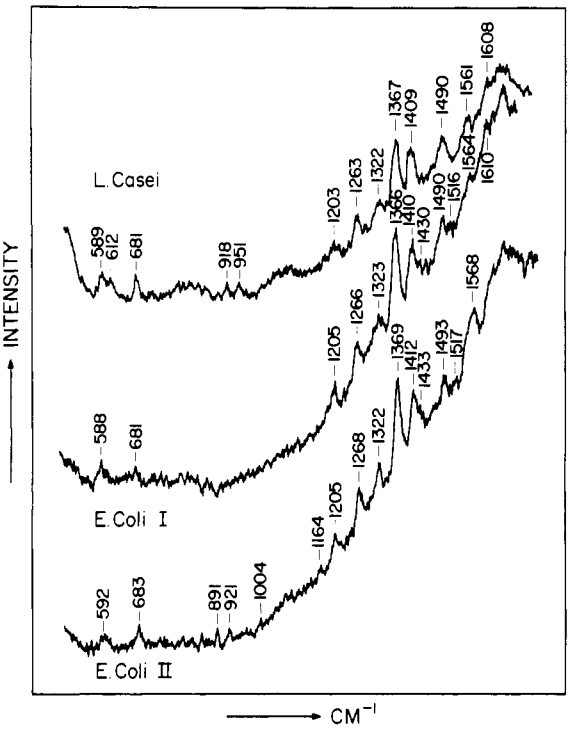

FIGURE 8: Comparison of the 350.6-nm excited resonance Raman spectra of methotrexate bound to a dihydrofolate reductase from three sources in the presence of cofactor NADPH, 5.5×10^{-5} M in enzyme, methotrexate, and NADPH, pH 7.0. For spectral conditions, see Experimental Procedures.

The addition of the cofactor NADPH to the MTX–enzyme complexes results in the 350.6-nm excited RR spectra shown in Figure 8. The binding within the ternary complexes is strong, and under the conditions of Figure 8 essentially all the MTX and NADPH molecules are bound to the enzyme (Dunn & King, 1980). At the level of signal-to-noise achieved in these experiments, the spectra of the ternary complexes are identical with those of the corresponding binary complexes. Since it is known that MTX binds more strongly in the ternary complex, it is apparent that the additional binding energy is not reflected in a major perturbation of MTX's vibrational energy states.

The 324-nm excited RR spectra of MTX bound to the three forms of DHFR were somewhat reduced in quality by a luminescent background (see, e.g., Figure 2, center). At this level of data quality, no differences could be found between peak positions in the RR spectra of the complexes by using DHFR from *E. coli* and *L. casei*. Moreover, no discernible changes in the spectra were brought about by addition of NADPH. Thus, the most intense modes of the *p*-aminobenzoyl group appear to be unperturbed by variation in enzyme source or addition of cofactors. On the basis of the analysis given above, however, it would be expected that the "amide features" near 1350 cm^{-1} which are thought to reflect changes in the benzoyl's amide linkage would be a good probe for small differences in the *p*-aminobenzoyl site. Unfortunately, the spectral quality is too poor in this region to follow spectral alterations with confidence.

References

Baccanari, D. P., Averett, D., Briggs, C., & Burchall, J. (1977) *Biochemistry 16*, 3566–3572.

Baker, B. R. (1959) *Cancer Chemother. Rep. 4*, 1–10.

Baker, B. R. (1967) *Design of Active-site Directed Irreversible Enzyme Inhibitors*, Chapter 10, Wiley, New York.

Blakley, R. L. (1969) *The Biochemistry of Folic Acid and Related Pteridines*, Chapter 5, North-Holland Publishing Co., Amsterdam.

Carey, P. R. (1978) *Q. Rev. Biophys. 11*, 309–370.

Cayley, P. J., Dunn, S. M. J., & King, R. W. (1981) *Biochemistry 20*, 874–879.

Charlton, P. A., Young, D. W., Birdsall, B., Feeney, J., & Roberts, G. C. K. (1979) *J. Chem. Soc., Chem. Commun.*, 922–924.

Collin, R., & Pullman, B. (1964) *Biochim. Biophys. Acta 89*, 232–241.

Dann, J. G., Ostler, G., Bjur, R. A., King, R. W., Scudder, P., Turner, P. C., Roberts, G. C. K., Burgen, A. S. V., & Harding, N. G. L. (1976) *Biochem. J. 157*, 559–571.

Dunn, S. M. J., & King, R. W. (1980) *Biochemistry 19*, 766–773.

Durig, J. R., Dunlap, R. B., & Gerson, D. J. (1980) *J. Raman Spectrosc. 9*, 266–272.

Erickson, J. S., & Matthews, L. K. (1972) *J. Biol. Chem. 247*, 5661–5667.

Hood, K. L., & Roberts, G. C. K. (1978) *Biochem. J. 171*, 357–366.

Kumar, K., & Carey, P. R. (1977) *Can. J. Chem. 55*, 1444–1453.

Kumar, K., King, R. W., & Carey, P. R. (1976) *Biochemistry 15*, 2195–2202.

Matthews, D. A., Alden, R. A., Bolin, J. T., Freer, J. T., Hamlin, R., Xuong, N., Kraut, J., Poe, M., Williams, M., & Hoogsteen, K. (1977) *Science (Washington, D.C.) 197*, 452–455.

Matthews, D. A., Alden, R. A., Bolin, J. T., Filman, D. J., Freer, S. T., Hamlin, R., Hol, W. G. J., Kisliuk, R. L., Pastore, E. J., Plante, L. T., Xuong, N., & Kraut, J. (1978) *J. Biol. Chem. 253*, 6946–6954.

Poe, M. (1973) *J. Biol. Chem. 248*, 7025–7032.

Poe, M., Greenfield, N. J., Hirshfield, J. M., & Hoogsteen, K. (1974) *Cancer Biochem. Biophys. 1*, 7–11.

Poe, M., Bennett, C. D., Donoghue, D., Hirshfield, J. M., Williams, M. N., & Hoogsteen, K. (1975) in *Chemistry and Biology of Pteridines* (Pfleiderer, W., Ed.) pp 51–58, de Gruyter, Berlin.

Roberts, G. C. K. (1978) *Ciba Found. Symp. 60*, 89.

Saperstein, D. D., Rein, A. J., Poe, M., & Leahy, M. F. (1978) *J. Am. Chem. Soc. 100*, 4296–4300.

Scheiner, S., & Kern, C. W. (1977) *J. Am. Chem. Soc. 99*, 7042–7050.